Relation between charge carrier mobility and lifetime in organic photovoltaics

Chellappan Vijila,[1,a)] Samarendra P. Singh,[2] Evan Williams,[1] Prashant Sonar,[1] Almantas Pivrikas,[3] Bronson Philippa,[4] Ronald White,[4] Elumalai Naveen Kumar,[5] S. Gomathy Sandhya,[1] Sergey Gorelik,[1] Jonathan Hobley,[1] Akihiro Furube,[6] Hiroyuki Matsuzaki,[6] and Ryuzi Katoh[7]

[1]*Institute of Materials Research and Engineering, A*STAR (Agency for Science, Technology and Research), 3 Research Link, Singapore 117602*
[2]*School of Natural Sciences, Shiv Nadar University, Gautam Buddha Nagar, India*
[3]*Centre for Organic Photonics and Electronics (COPE), The University of Queensland, Australia*
[4]*School of Engineering & Physical Sciences, James Cook University, Australia*
[5]*National University of Singapore, Singapore*
[6]*AIST, Japan*
[7]*Nihon University, Japan*

(Received 26 August 2013; accepted 22 October 2013; published online 13 November 2013)

The relationship between charge carrier lifetime and mobility in a bulk heterojunction based organic solar cell, utilizing diketopyrrolopyrole-naphthalene co-polymer and $PC_{71}BM$ in the photoactive blend layer, is investigated using the photoinduced charge extraction by linearly increasing voltage technique. Light intensity, delay time, and temperature dependent experiments are used to quantify the charge carrier mobility and density as well as the temperature dependence of both. From the saturation of photoinduced current at high laser intensities, it is shown that Langevin-type bimolecular recombination is present in the studied system. The charge carrier lifetime, especially in Langevin systems, is discussed to be an ambiguous and unreliable parameter to determine the performance of organic solar cells, because of the dependence of charge carrier lifetime on charge carrier density, mobility, and type of recombination. It is revealed that the relation between charge mobility (μ) and lifetime (τ) is inversely proportional, where the $\mu\tau$ product is independent of temperature. The results indicate that in photovoltaic systems with Langevin type bimolecular recombination, the strategies to increase the charge lifetime might not be beneficial because of an accompanying reduction in charge carrier mobility. Instead, the focus on non-Langevin mechanisms of recombination is crucial, because this allows an increase in the charge extraction rate by improving the carrier lifetime, density, and mobility simultaneously.
[http://dx.doi.org/10.1063/1.4829456]

I. INTRODUCTION

Bulk heterojunction (BHJ) based organic solar cells (OSCs) utilising blends of semiconducting polymers and fullerene derivatives have shown remarkable progress in terms of efficiency[1] and their ability to integrate into various novel applications such as liquid crystal displays (LCD)[2] and polarizers.[3] The power conversion efficiency (PCE) of BHJ based OSCs has already reached 10.6%, with continuing efforts on developing novel semiconducting polymers, device architectures and controlling the active film morphology.[4–6] In particular, the design of novel semiconducting polymers with beneficial properties is one of the major driving forces in order to overcome the challenges of device efficiency and stability for commercial applications. The desired material properties are: (i) broad absorption spectra to cover a wide range of the solar energy spectrum, (ii) tuned energy levels for efficient charge separation between the electron donor and acceptor material and to match with the work function of the electrodes, and (iii) good charge transport characteristics in the active layer to ensure efficient collection at the respective electrodes. As a result, various molecular structural optimization strategies have been adapted in the design of semiconducting polymers with enhanced planarity, solubility, and stability through the selection of suitable polymer backbones, side chains, and by tuning the electron donor (D) and acceptor (A) moieties in the polymer backbones.[7–10]

Generally, to utilize promising materials to their full extent, an enormous effort is required to optimise the device performance, such as varying the electron donor-acceptor compositions, solvent used for processing, film thickness, and annealing conditions as these factors can affect the film morphology significantly, which in turn affects the charge generation, transport, and recombination properties in the BHJ layer.[9,11–15] Efficient charge transport to the respective electrodes without recombination losses is one of the major requirements for improving the solar cell device performance. In P3HT:PCBM based BHJ solar cells, the increase of hole mobility and reduction in recombination rates, in the P3HT phase due to thermal annealing, strongly improved the

[a)]Author to whom correspondence should be addressed. Electronic mail: c-vijila@imre.a-star.edu.sg

device efficiency.[11] Moreover, the charge transport properties in the phase separated blend film differ significantly from their respective pristine films. For example, the hole mobility in a high performing low band gap polymer: poly(di(2-ethylhexyloxy)benzo[1,2-b:4,5-b′]dithiophene-co-octylthieno[3,4c] pyrrole-4,6-dione) (PBDTTPD) decreases by a factor of 7 when it is blended with PCBM due to few percolation pathways for holes in BHJ film compared to the pristine film.[11] The hole mobility in poly(2,5-bis(thiophene-2-yl)-(3,5-didecapentyldithieno[3,2-b;2′,3′-d] thiophene) (PBTDTT-15): $PC_{70}BM$ based BHJ film is almost an order of magnitude smaller compared to the hole mobility in the pristine film.[13] The charge recombination properties also show significant variation with respect to the donor/acceptor blend ratio, film thickness, the chemical nature of the hole and electron transporting material, as well as the blend morphology such as the size of the donor-acceptor domains, its purity and crystallinity.[12–16] This indicates that a detailed investigation of charge transport and recombination is essential with every new photovoltaic blend, as it could show significant variations in the underlying physics from the well-studied blends.

In this report, we investigated the relationship between the charge carrier mobility and lifetime in a low band gap semiconducting polymer (Poly{3,6-dithiophene-2-yl-2,5-di(2-octyldodecyl)-pyrrolo[3,4-c]pyrrole-1,4-dione-alt-naphthalene}) (PDPP-TNT) blended with C71-butyric acid methyl ester ($PC_{71}BM$). The PDPP-TNT:$PC_{71}BM$ (1:2) blend in a solvent mixture of chloroform: dichlorobenzene (DCB) [4:1 by volume] produces solar cell efficiencies of up to ~5%, although significant efforts have been devoted in order to improve the nanomorphology of the film through careful selection of solvents, composition ratios, and device architectures.[17–20] In addition, the absorption spectrum of the PDPP-TNT:$PC_{71}BM$ blend film covers the entire spectral range from 300 nm to 800 nm with a good charge mobility of around 1 cm^2/V s measured in organic thin-film transistor (OTFT) devices.[16,18] Moreover, the highest occupied molecular orbital (HOMO) and lowest unoccupied molecular orbital (LUMO) energy levels of PDPP-TNT are 5.29 eV and 3.79 eV, respectively, which are suitable for efficient charge separation with $PC_{71}BM$. Although this new generation low band gap semiconducting polymer PDPP-TNT fulfils the requirements for efficient solar cells applications, the limiting factors for achieving high performance are not very clear yet.

To further improve the understanding of this photovoltaic blend, detailed charge transport and recombination properties have been studied using photoinduced charge extraction by linearly increasing voltage (PhotoCELIV) technique. Measurements were conducted at varying temperatures, excitation light intensities, and delay times. The chemical structure of PDPP-TNT and $PC_{71}BM$, the absorption spectrum of the film with blend ratio of 1:2 (PDPP-TNT/$PC_{71}BM$), and the schematic diagram of the PhotoCELIV experiment are shown in Figure 1. The essence of this PhotoCELIV technique is the extraction of charge carriers generated by a laser pulse. The carrier density within the device, and the number of extracted charge carriers, can be varied by employing different laser intensities and different delay times (t_{del}) between the laser excitation and the voltage ramp. The detailed description of the experimental technique can be found elsewhere.[21,22]

II. EXPERIMENTAL SECTION

A. Device fabrication

The polymer PDPP–TNT (33 wt. %) and $PC_{71}BM$ (American Dye Source) (67 wt. %) was dissolved in a mixture of chloroform and o-dichlorobenzene (4:1 by volume)

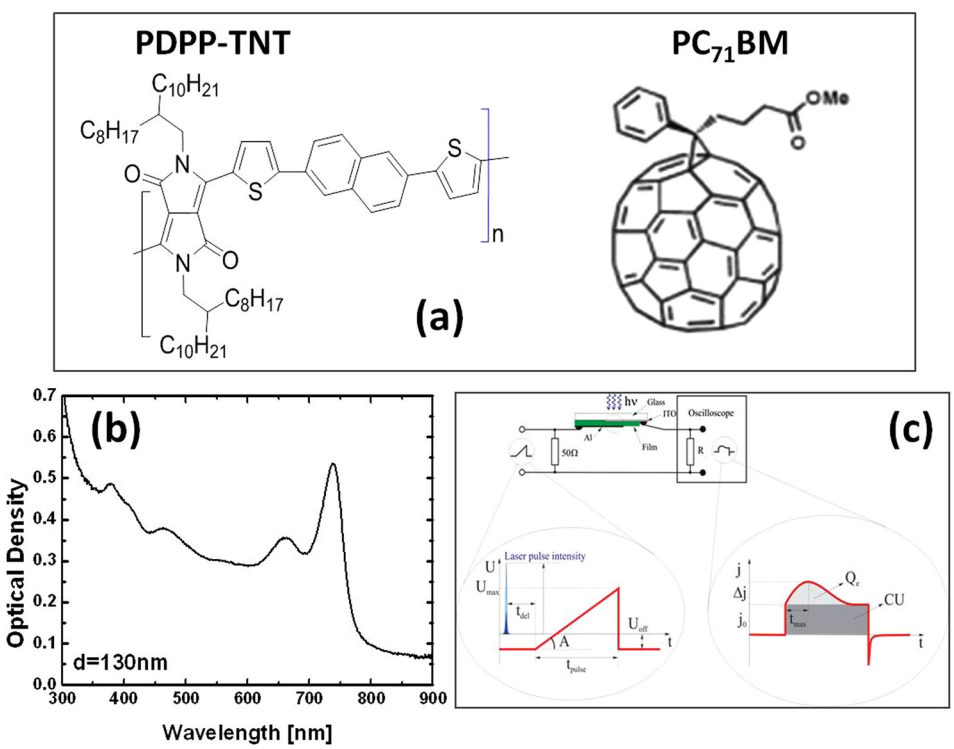

FIG. 1. (a) Chemical structure of PDPP-TNT and $PC_{71}BM$; (b) the absorption spectrum of the PDPP-TNT/$PC_{71}BM$ blend film with blend ratio (1:2); and (c) Schematic diagram of PhotoCELIV experiment. The essence of this technique is the extraction of photocarriers generated with laser pulse of different intensity and at various delay times t_{del}.

solvents. The solution was spin coated on a cleaned ITO-patterned glass substrate and the sample was then heated on a hot plate at 60 °C for 10 min in order to remove the excess solvent. A 100 nm thick aluminium electrode was deposited by thermal evaporation under a pressure of 10^{-5} mbar. The active area of the device was 0.04 cm^2 and the thickness of the film was found to be 170 nm measured using a KLA-Tencor P10 surface profiler. The film was also prepared on the quartz substrate for absorption spectral measurement. The detailed fabrication process optimizations were given elsewhere.[17,20]

B. PhotoCELIV measurement

The PhotoCELIV set-up consists of a pulsed Nd:YAG laser pumped OPO (Ekspla), pulse generator, function generator, and a digital oscilloscope. The sample was excited using the laser (pulse width <4 ns, pulse repetition rate 1 Hz) through the ITO side of the device. The laser wavelength of 740 nm with intensity of ~0.06 mJ/cm^2 was used for excitation. The measurement was carried out in the closed cycle helium cryostat by varying the temperatures and by varying the ramp rate of the applied voltage. The delay between the laser pulse and the voltage ramp was fixed to 2 μs. The photo-generated charge carriers were extracted using a linearly increasing voltage pulse of various amplitudes. The device built-in field was compensated by applying an offset voltage of around 0.5 V which is almost equivalent to the work function difference between the electrodes. The detailed PhotoCELIV measurement conditions were described somewhere else.[14,23] The charge carrier mobility and the density of photo-generated charge carriers were calculated from the time taken to reach the photocurrent maximum and by integrating the area under the photoinduced transients. The charge recombination behaviours were also studied by varying the intensity of the laser and delay time between the laser pulse and the voltage pulse. The charge carrier mobility was calculated using the modified relation recently proposed by Juska *et al.*[22] as shown in the following equation:

$$\mu = K^2 \frac{2d^2}{At_{max}^2}, \tag{1}$$

where d is the film thickness, t_{max} is the time at maximum extraction current (ΔJ_{max}), A is the voltage ramp rate, and K is the correction factor. The K value used in our calculation was 0.58 based on the estimation of average $\Delta J_{max}/J_0$ of 0.5 and αd at 740 nm of 1.6, respectively.[17] The charge carrier density was estimated by integrating the PhotoCELIV transients using the relation as shown in the following equation:[24]

$$p = \frac{2}{ed}\int_0^{\alpha} \Delta J dt, \tag{2}$$

where e is the elementary charge, $\int_0^{\alpha} \Delta J dt$ is the area under the photoinduced transients, and d is the film thickness.

III. RESULTS AND DISCUSSION

A. Laser intensity dependence of PhotoCELIV transients

To understand the charge recombination mechanism in the OPV device, the laser intensity dependence of PhotoCELIV transients were studied by varying the laser intensity from 0.025 mJ/cm^2 to 2.5 mJ/cm^2 using optical density filters. These studies were carried out at temperatures between 295 K and 120 K, because anomalies and deviations from Langevin-type recombination might be expected at temperatures much lower than room temperature. Figure 2(a) shows the PhotoCELIV transients at various light intensities and clearly reveals that the charge extraction peak saturates at high light intensities. Varied light intensity measurement can be used to determine the bimolecular recombination reduction factor β_L/β, where β is the actual, measured, recombination coefficient and $\boldsymbol{\beta_L = e(\mu_e + \mu_p)/\epsilon\epsilon_0}$ is the Langevin recombination coefficient which is dependent upon the charge carrier mobility (e is the elementary charge, ε is the dielectric constant, ε_0 is the vacuum permittivity, and μ_e and μ_p are the charge mobilities for electron and holes, respectively).[24,25] The ratio (β_L/β) or Langevin reduction factor can be directly obtained from the ratio between the photoresponse and displacement current $\Delta J_{max}/J_0$ (refer to Figure 1(c) for definitions).[26,27] In this study, $\Delta J_{max}/J_0$ was measured from the transients and plotted with respect to the

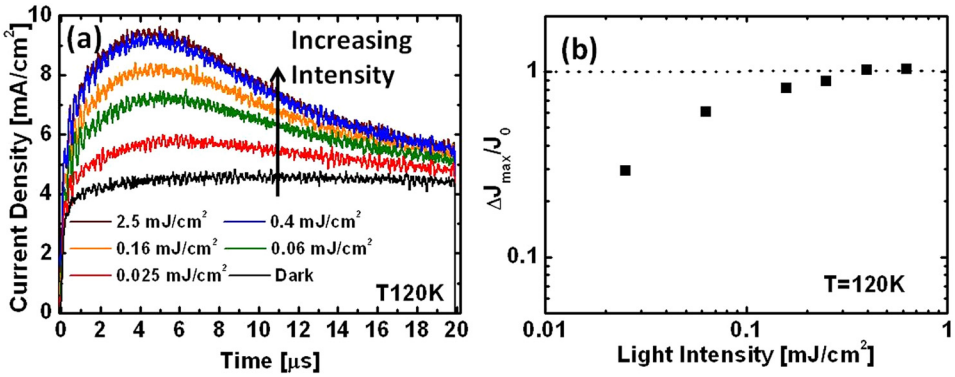

FIG. 2. (a) Laser intensity dependent photocurrent transient signals in Photo-CELIV experiment at low temperature (120 K). Transients demonstrate typical charge carrier extraction peaks even at low temperatures with clear saturation at highest laser intensities. (b) Variation of $\Delta J/J_0$ (refer Figure 1(c) for clarification) as a function of laser intensity at T = 120 K. The fact that $\Delta J/J_0$ saturates at highest laser intensities to one proves that bimolecular recombination is of Langevin type in studied solar cells even at low temperatures.

laser intensity as shown in Figure 2(b). It can be seen that $\Delta J_{max}/J_0$ approaches unity with increasing laser intensities and saturates at light intensities greater than 0.4 mJ/cm^2. It has already been shown numerically and experimentally in the literature that the saturation of $\Delta J_{max}/J_0$ to unity directly indicates the Langevin type bimolecular recombination, whereas the Non-Langevin system allows extraction of more charges than the capacitor limit.[24–27] Therefore, the saturation of ΔJ_{max} to a value equal to J_0 at high light intensities directly proves that the bimolecular recombination is of the Langevin type in the studied solar cell using the PDPP-TNT:$PC_{71}BM$ blend. The bimolecular recombination is detrimental for charge extraction efficiency. It has been reported that the increase in active layer thickness of low band gap polymer based BHJ, decreases the external quantum efficiency due to bimolecular recombination losses. The bimolecular recombination is more significant in 300 nm thick film than the optimal 100 nm thick film and the cause for the bimolecular recombination loss is the slow hole mobility due to low degree of polymer ordering in the blend film compared to the pristine film.[12] Using the charge mobility measured for PDPP-TNT:$PC_{71}BM$ at 120 K of $\sim 5 \times 10^{-5}$cm^2/V s, and dielectric constant of 3.9, the $\boldsymbol{\beta_L}$ value estimated was 2×10^{-11} cm^3/s, which is 2 orders of magnitude higher than the bimolecular recombination coefficient reported for the P3HT:PCBM (2×10^{-13} cm^3/s) blend at room temperature.[24] The β_L for PDPP-TNT:$PC_{71}BM$ at room temperature is 3.3×10^{-10} cm^3/s due to the increase of carrier mobility (7×10^{-4}cm^2/V s) with temperature. The Langevin type recombination has also been reported for several photovoltaic blends such as MDMO-PPV:PCBM,[28,29] and the low band gap polymer poly[2,6-(4,4-bis-{2-ethylhexyl}-4H-cyclopenta[2,1-b;3,4-b0]-dithiophene)-alt-4,7-(2,1,3-benzothiadiazole)]:$PC_{71}BM$,[30,31] where the value of β_L/β was found to be 1.3, closer to the Langevin rate.[26–29] In general, the homogeneous materials system or the blend film with small donor-acceptor domain sizes and equal electron and hole mobilities, the bimolecular recombination can be described completely by β_L. The recombination rate constant for average domain size of 35 nm shows greater deviation from β_L than the average domain size of 4 nm.[32] The bimolecular recombination rate (β) is reduced in several photovoltaic blends such as PBTDTT-15:$PC_{71}BM$[14] and P3HT:PCBM,[24] where the measured β is a few orders of magnitude lower compared to β_L. The reduced β is attributed to the strongly phase separated morphology and the formation of two dimensional lamellar structures or pure domains of donor and acceptor materials.[26,32]

B. Temperature dependence of charge mobility

The variation of charge mobility with temperature has been studied by measuring the PhotoCELIV transients for a temperature range of 120 K to 295 K, with a fixed voltage ramp rate of 3×10^5 V/s and laser delay of 2 μs. The charge mobility at 295 K was found to be 7×10^{-4}cm^2/V s that decreased to 5×10^{-5}cm^2/V s at 120 K. The results indicate that the charge mobility is temperature dependent, with higher temperatures corresponding to higher mobilities. The temperature dependence of μ has been analysed according to the Arrhenius behaviour ($\mu = \mu_0 \exp(-\Delta E/kT)$, and the disorder formalism ($\mu = \mu_0 \exp(-2\sigma/3kT)^2$), where ΔE is an activation energy, k is the Boltzmann constant, μ_0 is the mobility pre-factor, and σ is the energy disorder parameter or the width of the Gaussian density of states.[33,34] The plot of $\ln(\mu)$ versus 1/T and $1/T^2$ is shown in Figure 3. The solid lines are the fits according to the Arrhenius form and the disorder formalism. It can be seen that the $\ln(\mu)$ versus 1/T plot shows linear relationship and the slope and the intercept of the plot yielded an activation energy of 48 meV and mobility pre-factor of $\mu_0 = 4 \times 10^{-3}$ cm^2/V s, respectively.

According to the disorder formalism, the charge mobility increases with increasing temperature as the charge transport is governed by a thermally assisted hopping process between localized charge transport sites. The energetic distribution of these localized sites follows a Gaussian shape with width σ, which provides a measure of the degree of energetic disorder in the system. The disorders in organic semiconductors arise from material impurity, variation in the conjugation length, twisting or bending of the polymer chain, and morphological inhomogenities. With the presence of energetic disorder in the material, the charge carriers are delayed by energy barriers between subsequent hops while migrating through the sample. These barriers are more readily overcome at higher temperatures, since the hopping is assisted by thermal energy. The slope of $\ln(\mu)$ versus $1/T^2$ plot (shown in Figure 3) provides the width of the density of states, σ. The value of σ and the mobility pre-factor (μ_0) obtained from the fit was $\sim$30 meV and 1×10^{-3}cm^2/V s, respectively. It was noted that the $\ln(\mu)$ versus $1/T^2$ plot was not linear at low temperatures <220 K. The σ value estimated by fitting the temperature range of 220 K–295 K was $\sim$40 meV with a μ_0 value of $\sim 2 \times 10^{-3}$cm^2/V s.

C. Estimation of charge carrier lifetime from laser delay dependence of PhotoCELIV transients

To understand the charge recombination behavior, PhotoCELIV transients were measured at varying laser delays

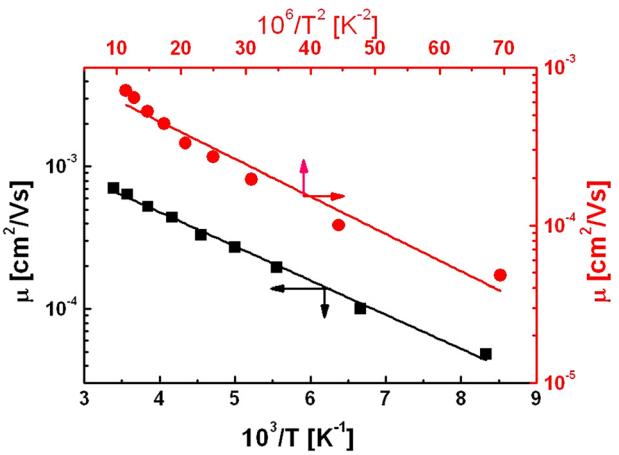

FIG. 3. Charge carrier mobility as a function of $10^3/T$ (squares) and $10^6/T^2$ (circles). The solid lines are the linear fit, the activation energy (ΔE) and energy disorder parameter (σ) obtained from the slope of the fit was found to be 48 meV and 30 meV, respectively.

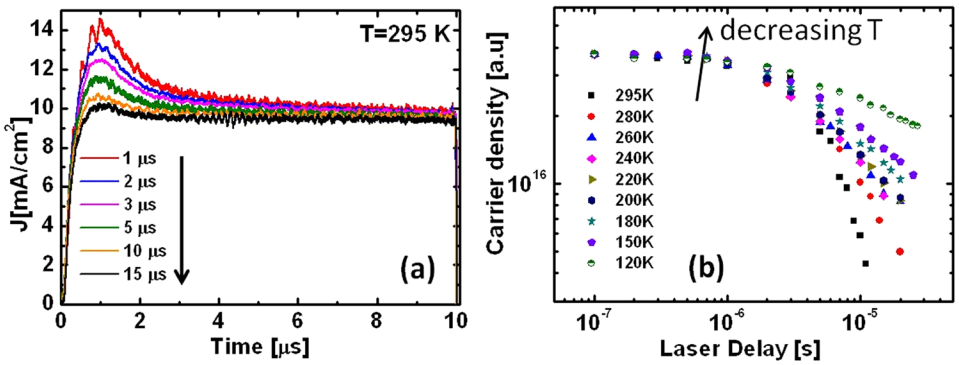

FIG. 4. (a) Photocurrent transient signals in PhotoCELIV experiment recorded at room temperature for different delay times between laser and extracting pulses. By integrating the photocurrent related part of transient signal, the photoinduced carrier density as a function of delay time is estimated and shown in (b) for various temperatures. Due to longer charge carrier lifetime at lower temperatures, the concentration decay extends to longer time scales.

for temperatures between 120 K and 295 K. The results at 295 K are shown in Figure 4(a). It can be seen clearly in Figure 4(a) that the photogenerated current disappears very quickly with respect to the increasing laser delay times at 295 K, indicating a short charge carrier lifetime. The photoinduced charge carriers can only be extracted up to 15 μs delay after the laser excitation, which is significantly shorter than the reported values for photovoltaic blends such as MDMOPPV/PCBM,[28,29] PBTDTT-15/$PC_{70}BM$,[14] and P3HT/PCBM,[26] where the charge extraction is possible up to several ms after laser excitation. The charge carrier concentration was calculated by integrating the PhotoCELIV transients and subtracting the capacitive displacement current. A detailed description of the calculation of carrier density is given in the experimental Section II B. The variation of charge carrier concentration with respect to the laser delay for different temperatures is shown in Figure 4(b). The charge carrier concentration decreases with increasing laser delay due to recombination; however, the decay rate is slower at low temperatures compared to room temperature, indicating the temperature dependence of the recombination rate. The concentration dependent charge carrier lifetime (τ) was estimated from the time at which the carrier density drops to 50% of its initial value. The charge carrier lifetime estimated at 295 K was 3 μs, which increased to $\sim$20 μs at 120 K. The variation of charge carrier lifetime and mobility with temperature is shown in Figure 5(a). It can be seen that the charge mobility is directly proportional to temperature whereas the charge carrier lifetime is inversely proportional to temperature. The increase of carrier lifetime at low temperatures is predicted by the classical Langevin theory, because lower temperatures reduce the mobility, which in turn reduces the rate at which carriers can physically meet for recombination. Conversely, a higher mobility increases the probability of finding the opposite charge carrier and hence enhances the charge recombination. Therefore, according to the Langevin theory, the recombination rate in PDPP-TNT:$PC_{71}BM$ is directly proportional to the charge carrier mobility. This theory predicts that the mobility lifetime product ($\mu\tau$) should be independent of temperature. The $\mu\tau$ product, plotted in Figure 5(b), agrees with this prediction within the range of the experimental accuracy. The $\mu\tau$ value ($\sim 3 \times 10^{-9}$ cm^2/V) obtained for PDPP-TNT/$PC_{71}BM$ in this study is comparable to the value recently reported for PCDTBT:$PC_{71}BM$.[35] Although the charge mobility of PDPP-TNT:$PC_{71}BM$ at 295 K is comparable to that of the P3HT/PCBM blend, the shorter carrier lifetime in PDPP-TNT:$PC_{71}BM$ lowers its $\mu\tau$ product. Therefore, the obtained results clearly demonstrate that the bimolecular recombination loss is one of the major device efficiency limiting factors in PDPP-TNT:$PC_{71}BM$ blends. In photovoltaic systems with Langevin type bimolecular recombination, strategies to increase the charge lifetime without changing the recombination mechanism might not be beneficial, because of the corresponding reduction in charge carrier mobility. Instead, it is crucial to focus on non-Langevin mechanisms of recombination, as these eliminate the trade-off between lifetime and mobility. In non-Langevin systems, the charge extraction rate can be increased by improving the carrier lifetime, carrier density and mobility simultaneously, without the need to optimise contradictory objectives.

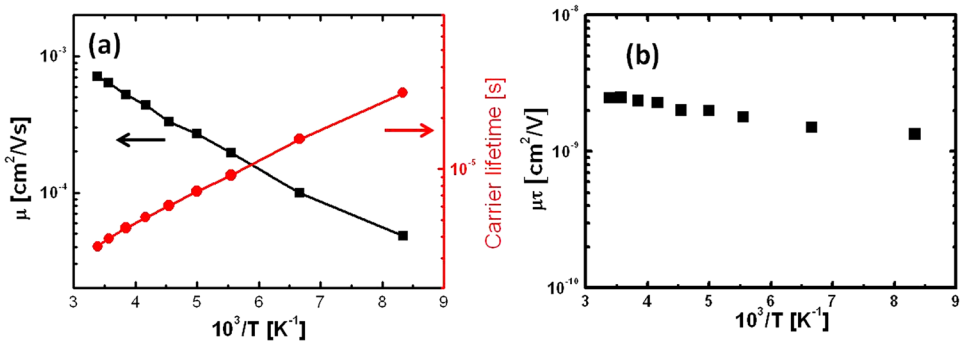

FIG. 5. (a) Charge carrier half-decay lifetime measured from concentration decay (shown in Figure 4(b)) and charge mobility (shown in Figure 3(a)) and (b) shows mobility-lifetime product $\mu\tau_\beta$ in the range of studied temperatures. Temperature independent $\mu\tau_\beta$ product shows that reduction in charge carrier mobility results in longer carrier lifetime, as expected in Langevin-type bimolecular recombination, where the recombination rate is determined by their movement velocity (charge mobility).

IV. CONCLUSION

The charge mobility, charge carrier concentration, and carrier lifetime in a BHJ photoactive layer consisting of a new low band gap semiconducting polymer were studied in detail. The results indicated that the charge recombination in PDPP-TNT:$PC_{71}BM$ follows the classical Langevin theory, where the charge recombination rate is directly proportional to charge mobility. We have also shown that the charge mobility and charge carrier lifetime are inversely proportional to each other and the product of charge mobility and lifetime ($\mu\tau$) is independent of temperature, in complete agreement with the theoretical prediction. The obtained results proved that in photovoltaic systems with Langevin type recombination, strategies to increase the carrier lifetime or charge mobility alone are not beneficial as the improvement of one parameter causes a decrease in the other parameter. In order to improve the device performance, it is important to focus on non-Langevin type systems, where the carrier extraction efficiency can be enhanced through the simultaneous improvement of carrier lifetime, carrier density and mobility.

ACKNOWLEDGMENTS

This work was funded by the A*STAR-JST Strategic International Cooperative Programme (1st Joint Grant Call—Project No. 1021630071).

[1]J. You, L. Dou, K. Yoshimura, T. Kato, K. Ohya, T. Moriarty, K. Emery, C. Chen, J. Gao, G. Li, and Y. Yang, Nat. Commun. **4**, 1446 (2013).
[2]R. Zhu, A. Kumar, and Y. Yang, Adv. Mater. **23**, 4193 (2011).
[3]H. J. Park, T. Xu, J. Y. Lee, A. Ledbetter, and L. J. Guo, ACS Nano **5**, 7055 (2011).
[4]S. Sista, Adv. Mater. **22**, 380 (2010).
[5]S. H. Park, A. Roy, S. Beaupre, S. Cho, N. Coates, J. S. Moon, D. Moses, M. Leclerc, K. Lee, and A. J. Heeger, Nature Photon. **69**, 1 (2009).
[6]Y. Liang, Z. Xu, J. Xia, S. T. Tsai, Y. Wu, G. Li, C. Ray, and L. Yu, Adv. Mater. **22**, E135 (2010).
[7]S. C. Price, A. C. Stuart, L. Q. Yang, H. X. Zhou, and W. You, J. Am. Chem. Soc. **133**, 4625 (2011).
[8]D. A. M. Egbe, E. Tekin, E. Birckner, A. Pivrikas, N. S. Sariciftci, and U. S. Schubert, Macromolecules **40**, 7786 (2007).
[9]G. Adam, A. Pivrikas, A. M. Ramil, S. Tadesse, T. Yohannes, N. S. Sariciftci, and D. A. M. Egbe, J. Mater. Chem. **21**, 2594 (2011).
[10]M. C. Chen, D. Liaw, W. Chen, Y. Huang, J. Sharma, and Y. Tai, Appl. Phys. Lett. **99**, 223305 (2011).
[11]Y. Kim, S. Cook, S. M. Tuladhar, S. A. Choulis, J. Nelson, J. R. Durrant, D. D. C. Bradley, M. Giles, I. Mcculloch, C. S. Ha, and M. Ree, Nature Mater. **5**, 197 (2006).
[12]J. A. Bartelt, Z. M. Beiley, E. T. Hoke, W. R. Mateker, J. D. Douglas, B. A. Collins, J. R. Tumbleston, K. R. Graham, A. Amassian, H. Ade, J. M. J. Fréchet, M. F. Toney, and M. D. McGehee, Adv. Energy Mater. **3**, 364 (2013).
[13]V. D. Mihailetchi, L. J. A. Koster, P. W. M. Blom, C. Melzer, B. de Boer, J. K. J. Van Duren, and R. A. J. Janssen, Adv. Funct. Mater. **15**, 795 (2005).
[14]T. Mein Jin, G. Wei Peng, L. Jun, G. Pundir, C. Vijila, and C. Zhikuan, ACS Appl. Mater. Interfaces **2**, 1414 (2010).
[15]D. H. K. Murthy, A. Melianas, Z. Tang, G. Juška, K. Arlauskas, F. Zhang, L. D. A. Siebbeles, O. Inganäs, and T. J. Savenije, Adv. Funct. Mater. **23**, 4262 (2013).
[16]H. Azimi, A. Senes, M. C. Scharber, K. Hingerl, and C. J. Brabec, Adv. Energy Mater. **1**, 1162 (2011).
[17]P. Sonar, S. P. Singh, Y. Li, Z. E. Ooi, T.-J. Ha, I. Wong, S. M. Siang, and A. Dodabalapur, Energy Environ. Sci. **4**, 2288 (2011).
[18]J. Ajuria, S. Chavhan, R. T. Zaera, J. Chen, A. J. Rondinone, P. Sonar, A. Dodabalapur, and R. Pacios, Organ. Electron. **14**, 326 (2013).
[19]T. J. Ha, P. Sonar, and A. Dodabalapur, Appl. Phys. Lett. **98**, 253305 (2011).
[20]E. L. Williams, S. Gorelik, I. Y. Phang, M. Bosman, C. Vijila, G. S. Subramanian, P. Sonar, J. Hobley, S. P. Singh, H. Matsuzaki, A. Furube, and R. Katoh, RSC Adv. **3**, 20113 (2013).
[21]G. Juska, K. Arlauskas, M. Viliunas, and J. Kocka, Phys. Rev. Lett. **84**, 4946 (2000).
[22]G. Juska, N. Nekrasas, V. Valentinavicius, P. Meredith, and A. Pivrikas, Phys. Rev B. **84**, 155202 (2011).
[23]C. Vijila, G. M. Ng, T. Mein Jin, G. Wei-Peng, and F. Zhu, Appl. Phys. Lett. **95**, 263305 (2009).
[24]A. Pivrikas, N. S. Sariciftci, G. Juska, and R. Osterbacka, Prog. Photovoltaics **15**, 677 (2007).
[25]A. Pivrikas, G. Juška, R. Österbacka, M. Westerling, M. Viliunas, K. Arlauskas, and H. Stubb, Phys. Rev. B. **71**, 125205 (2005).
[26]A. Pivrikas, G. Juska, A. J. Mozer, M. Scharber, K. Arlauskas, N. S. Sariciftci, H. Stubb, and R. Osterbacka, Phys. Rev. Lett. **94**, 176806 (2005).
[27]A. Armin, G. Juska, B. W. Philippa, P. L. Burn, P. Meredith, R. D. White, and A. Pivrikas, Adv. Energy Mater. **3**, 321 (2013).
[28]G. Denler, A. J. Mozer, G. Juska, A. Pivrikas, R. Osterbacka, A. Fuchsbaur, and N. S. Sariciftci, Org. Electron. **7**, 229 (2006).
[29]A. J. Mozer, N. S. Sariciftci, A. Pivrikas, R. Österbacka, G. Juška, L. Brassat, and H. Bässler, Phys. Rev B. **71**, 035214 (2005).
[30]A. Pivrikas, H. Neugebauer, and N. S. Sariciftci, IEEE J. Sel. Top. Quantum Electron. **16**, 1746 (2010).
[31]A. Armin, M. Velusamy, P. L. Burn, P. Meredith, and A. Pivrikas, Appl. Phys. Lett. **101**, 083306 (2012).
[32]C. Groves and N. C. Greenham, Phys. Rev. B **78**, 155205 (2008).
[33]C. Vijila, A. Pivrikas, H. Chun, C. Zhikuan, R. Österbacka, and C. Soo Jin, Org. Electron. **8**, 8 (2007).
[34]W. Tang, C. Vijila, M. Liu, Z. K. Chen, and L. Ke, ACS Appl. Mater. Interfaces **1**, 1467 (2009).
[35]A. Baumann, J. Lorrmann, D. Rauh, C. Deibel, and V. Dyakonov, Adv. Mater. **24**, 4381 (2012).